JNS

CLINICAL ARTICLE

Characterizing tumor invasiveness of glioblastoma using multiparametric magnetic resonance imaging

Chao Li, MD, PhD,[1,2] Shuo Wang, PhD,[3] Jiun-Lin Yan, MD, PhD,[1,4,5] Turid Torheim, PhD,[6,7] Natalie R. Boonzaier, PhD,[1,8] Rohitashwa Sinha, MRCS,[1] Tomasz Matys, PhD, FRCR,[3,9] Florian Markowetz, PhD,[6,7] and Stephen J. Price, PhD, FRCS[1,10]

[1]Cambridge Brain Tumor Imaging Laboratory, Division of Neurosurgery, Department of Clinical Neurosciences, [3]Department of Radiology, [6]Cancer Research UK Cambridge Institute, and [10]Wolfson Brain Imaging Centre, Department of Clinical Neurosciences, University of Cambridge, United Kingdom; [2]Department of Neurosurgery, Shanghai General Hospital, Shanghai Jiao Tong University School of Medicine, Shanghai, China; [4]Department of Neurosurgery, Chang Gung Memorial Hospital, Keelung, Taiwan; [5]Chang Gung University College of Medicine, Taoyuan, Taiwan; [7]CRUK & EPSRC Cancer Imaging Centre in Cambridge and Manchester, Cambridge; [8]Developmental Imaging and Biophysics Section, Great Ormond Street Institute of Child Health, University College London; and [9]Cancer Trials Unit, Department of Oncology, Addenbrooke's Hospital, Cambridge, United Kingdom

OBJECTIVE The objective of this study was to characterize the abnormalities revealed by diffusion tensor imaging (DTI) using MR spectroscopy (MRS) and perfusion imaging, and to evaluate the prognostic value of a proposed quantitative measure of tumor invasiveness by combining contrast-enhancing (CE) and DTI abnormalities in patients with glioblastoma.

METHODS Eighty-four patients with glioblastoma were recruited preoperatively. DTI was decomposed into isotropic (p) and anisotropic (q) components. The relative cerebral blood volume (rCBV) was calculated from the dynamic susceptibility contrast imaging. Values of *N*-acetylaspartate, myoinositol, choline (Cho), lactate (Lac), and glutamate + glutamine (Glx) were measured from multivoxel MRS and normalized as ratios to creatine (Cr). Tumor regions of interest (ROIs) were manually segmented from the CE T1-weighted (CE-ROI) and DTI-q (q-ROI) maps. Perfusion and metabolic characteristics of these ROIs were measured and compared. The relative invasiveness coefficient (RIC) was calculated as a ratio of the characteristic radii of CE-ROI and q-ROI. The prognostic significance of RIC was tested using Kaplan-Meier and multivariate Cox regression analyses.

RESULTS The Cho/Cr, Lac/Cr, and Glx/Cr in q-ROI were significantly higher than CE-ROI ($p = 0.004$, $p = 0.005$, and $p = 0.007$, respectively). CE-ROI had significantly higher rCBV values than q-ROI ($p < 0.001$). A higher RIC was associated with worse survival in a multivariate overall survival (OS) model (hazard ratio [HR] 1.40, 95% confidence interval [CI] 1.06–1.85, $p = 0.016$) and progression-free survival (PFS) model (HR 1.55, 95% CI 1.16–2.07, $p = 0.003$). An RIC cutoff value of 0.89 significantly predicted shorter OS (median 384 vs 605 days, $p = 0.002$) and PFS (median 244 vs 406 days, $p = 0.001$).

CONCLUSIONS DTI-q abnormalities displayed higher tumor load and hypoxic signatures compared with CE abnormalities, whereas CE regions potentially represented the tumor proliferation edge. Integrating the extents of invasion visualized by DTI-q and CE images into clinical practice may lead to improved treatment efficacy.

https://thejns.org/doi/abs/10.3171/2018.12.JNS182926

KEYWORDS glioblastoma; MRI; diffusion tensor imaging; magnetic resonance spectroscopy; prognosis; oncology; perfusion imaging

ABBREVIATIONS 5-ALA = 5-aminolevulinic acid; CE = contrast enhancing; Cho = choline; CI = confidence interval; Cr = creatine; CSI = chemical shift imaging; DSC = dynamic susceptibility contrast-enhancement; DTI = diffusion tensor imaging; DTI-p = DTI-isotropic; DTI-q = DTI-anisotropic; EOR = extent of resection; FSL = Functional MRI of the Brain Software Library; Glx = glutamate + glutamine; HR = hazard ratio; IDH-1 = isocitrate dehydrogenase 1; Lac = lactate; MGMT = *O*-6-methylguanine-DNA methyltransferase; mIns = myoinositol; MRS = magnetic resonance spectroscopy; NAA = *N*-acetylaspartate; NAWM = normal-appearing white matter; OS = overall survival; PFS = progression-free survival; rCBV = relative cerebral blood volume; RIC = relative invasiveness coefficient; ROI = region of interest.

SUBMITTED October 22, 2018. **ACCEPTED** December 26, 2018.
INCLUDE WHEN CITING Published online April 26, 2019; DOI: 10.3171/2018.12.JNS182926.

Glioblastomas are the most common malignant brain tumors in adults, characterized by dismal patient survival. Although maximal safe resection followed by radiotherapy with concomitant and adjuvant temozolomide chemoradiotherapy has improved patient outcomes, the median overall survival (OS) remains 12–15 months.[3] Accumulating evidence suggests that aggressive resection can prolong patient survival.[8,24] However, extended resection or escalating adjuvant radiation volume may subject the patient to a higher risk of neurological deficits. A more accurate targeting of the tumor with less risk of functional damage to patients is therefore crucial for treatment planning.

MRI is widely used in monitoring the disease and defining the tumor region. In current clinical practice, contrast-enhancing (CE) T1-weighted imaging is considered the gold standard for planning surgery and radiotherapy. Glioblastoma is characterized by its infiltration into the surrounding brain tissue. Thus, infiltrative tumor cells are well known beyond the CE region.[19] Other conventional sequences, including T2-weighted imaging and FLAIR, are nonspecific in differentiating tumor invasion from peritumoral edema and treatment effects that cause white matter change.[28]

Many MRI methods have been developed that provide signals relating to pathological changes in the tumor.[16] Diffusion tensor imaging (DTI) measures the magnitude and direction of water mobility and is sensitive to detecting tumor invasion that leads to the disruption of brain microstructure.[15,23] Previous work has shown that the diffusion tensor can be decomposed into isotropic (DTI-p) and anisotropic (DTI-q) components.[14] The resulting DTI-p and -q maps have potential in delineating tumor invasion.[6,19] Image-guided biopsy studies have shown that DTI-q abnormalities represent regions of higher tumor burden.[19] A recent retrospective study revealed that more extensive resection of DTI-q and CE abnormalities was associated with improved patient outcome, suggesting both abnormality areas could be clinically relevant.[29]

The first purpose of this study was to compare the pretreatment DTI-q and CE abnormalities using magnetic resonance spectroscopy (MRS) and perfusion imaging in treatment-naive patients. As DTI-q may represent a tumor region with high tumor load, we hypothesized that the DTI-q abnormality would represent a more hypoxic region resulting from the higher cellularity in this region. On the other hand, because contrast enhancement is associated with contrast agent leakage, we hypothesized that the CE abnormality may represent a region with more evidence of neovascularization, indicated by the aberrant perfusion.

The second purpose of this study was to evaluate the prognostic value of a quantitative measure of tumor invasiveness, in which we integrated both volumes of DTI-q and CE abnormalities. Various studies have shown that hypoxia may be a factor driving tumor progression.[2] Furthermore, angiogenesis can be activated by hypoxia through a series of proangiogenic factors, leading to neovascularization during tumor expansion.[4] Therefore, we hypothesized that combining both DTI-q and CE abnormalities could be of prognostic value.

Methods

Patient Population

Patients with a suspected diagnosis of supratentorial newly diagnosed glioblastoma were prospectively recruited from July 2010 to August 2015. All patients were required to have a good performance status (WHO performance status 0–1) before surgery. Patients who had a history of a previous brain tumor, cranial surgery, radiotherapy/chemotherapy, or contraindication for MRI were excluded. This study was approved by the Cambridgeshire 2 LREC Ethical Committee. Signed informed consent was obtained from each patient.

Treatment and Response Assessment

Neuronavigation (StealthStation, Medtronic) and 5-aminolevulinic acid (5-ALA) fluorescence were used to guide surgery, with other adjuvants (e.g., cortical and subcortical mapping) to allow maximal safe resection when appropriate. Extent of resection (EOR) was assessed according to the postoperative MRI within 72 hours and classified as complete resection of enhancing tumor, partial resection of enhancing tumor, or biopsy.[27] Patient treatment response was evaluated according to the Response Assessment in Neuro-Oncology criteria,[28] which incorporate clinical and radiological measurements for assessment. All MRI and histological data were collected prospectively. In some cases, pseudoprogression was suspected when new enhancement was observed within 12 weeks after radiotherapy. In these cases, the patient's treatment was continued, and true progression or pseudoprogression was determined retrospectively.

Preoperative MRI Acquisition

All MRI sequences were performed on a 3-T MRI system (Magnetron Trio; Siemens Healthcare) with a standard 12-channel receive-head coil.[7] MRI sequences were acquired as follows: postcontrast T1-weighted sequence (TR/TE/TI 2300/2.98/900 msec, flip angle 9°, FOV 256 × 240 mm, 176–208 slices, no slice gap, and voxel size 1.0 × 1.0 × 1.0 mm) after intravenous injection of 9 ml of gadobutrol (1.0 mmol/ml, Bayer); T2-weighted sequence (TR/TE 4840–5470/114 msec, refocusing pulse flip angle 150°, FOV 220 × 165 mm, 23–26 slices, 0.5-mm slice gap, and voxel size 0.7 × 0.7 × 5.0 mm); and T2-weighted FLAIR (TR/TE/TI 7840–8420/95/2500 msec, refocusing pulse flip angle 150°, FOV 250 × 200 mm, 27 slices, 1-mm slice gap, and voxel size 0.78125 × 0.78125 × 4.0 mm). Perfusion-weighted imaging was acquired with a dynamic susceptibility contrast-enhancement (DSC) sequence (TR/TE 1500/30 msec, flip angle 90°, FOV 192 × 192 mm, 19 slices, 1.5-mm slice gap, and voxel size 2.0 × 2.0 × 5.0 mm) with 9 ml of gadobutrol (1.0 mmol/ml) followed by a 20-ml saline flush administered via a power injector at 5 ml/sec. DTI was acquired before contrast imaging, using a single-shot echo-planar sequence (TR/TE 8300/98 msec, flip angle 90°, FOV 192 × 192 mm, 63 slices, no slice gap, and voxel size 2.0 × 2.0 × 2.0 mm); inline apparent diffusion coefficient calculation was performed during DTI acquisition using b values of 0–1000 sec/mm^2. Multivoxel 2D ^{1}H-MRS chemical shift imaging (CSI) utilized

a semi-LASER sequence (TR/TE 2000/30–35 msec, flip angle 90°, FOV 160 × 160 mm, and voxel size 10 × 10 × 15–20 mm). Point-resolved spectroscopy excitation was selected to encompass a grid of 8 rows × 8 columns on T2-weighted images.

Imaging Processing

All other sequences were coregistered to the T2-weighted images, which were used to plan the CSI in each subject. The coregistration was performed using the linear image registration tool functions in Oxford Centre for Functional MRI of the Brain Software Library (FSL; version 5.0.0).[22] DSC processing and leakage correction were performed with the NordicICE software (NordicNeuroLab), in which the arterial input function was automatically defined. The relative cerebral blood volume (rCBV) maps were calculated. DTI images were processed using the diffusion toolbox in FSL,[1] during which normalization and eddy current correction were performed. The decomposition of processed DTI images into isotropic components (p) and anisotropic components (q) was performed using a previously described method.[14]

Regions of Interest

Tumor regions of interest (ROIs) were manually segmented on the coregistered CE T1-weighted and DTI-q images. The delineation was independently performed blinded to the outcome by the authors with fair agreement (Fig. 1).[6,29] To compare the imaging characteristics, a Boolean subtraction of CE and p abnormalities was performed in MATLAB (MathWorks) to obtain the CE-ROI (without DTI-q abnormality) and the q-ROI (anisotropic ROI).

For each individual patient, normal-appearing white matter (NAWM) regions were drawn manually in the contralateral white matter as normal controls. Each voxel value in the ROIs was normalized by dividing it by the mean voxel value of the contralateral NAWM.

Tumor Characteristic Radius

To quantify the extent of irregular tumors in 3D space, the characteristic radius of ROIs was calculated using a previously reported method.[10] Briefly, the smallest bounding ellipsoid was fitted to the whole tumor volume revealed by ROIs. The length of this ellipsoid's semimajor axis was used to measure the characteristic radius of tumor ROI. We then calculated the ratio of CE characteristic radius to DTI-q characteristic radius, as a relative invasiveness coefficient (RIC). A demonstration of the calculation of characteristic radius and RIC is provided (Fig. 2).

Multivoxel MRS Processing

CSI data were processed using LCModel (Provencher).[7] All the concentrations of metabolites were calculated as a ratio to creatine (Cr).[5] All relevant spectra from CSI voxels of interest were assessed for artifacts using previously described criteria.[20] The values of the Cramer-Rao lower bounds were used to evaluate the quality and reliability of CSI data and values with standard deviations > 20% were discarded.[20]

Because the CSI was planned on T2 space and CSI images have lower spatial resolution than T2 images, to account for the difference in resolution, all tumor pixels in T2 space were projected to CSI space according to their coordinates using MATLAB. The proportion of T2-space tumor pixels occupying each CSI voxel was calculated. Only CSI voxels that were completely located within tumor ROIs were included for further analysis. The weight of each CSI voxel was taken as the proportion of the tumor pixels in that CSI voxel. The weighted sum value was used as the final metabolic value of the tumor ROIs.

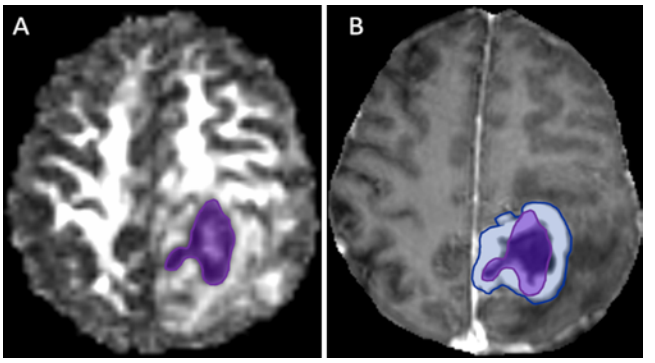

FIG. 1. A demonstration of ROIs in a DTI-q image (**A**) and postcontrast T1-weighted image (**B**). The q-ROI (*purple*) shows the abnormality revealed on a DTI-q map. The CE-ROI (*blue*) is a CE tumor region excluding the DTI-q abnormality. Figure is available in color online only.

Statistical Analysis

All statistical analyses were performed in RStudio (version 3.2.3). The CSI data and rCBV values were compared with pairwise Kruskal-Wallis rank-sum tests using the Benjamini-Hochberg procedure to control the false discovery rate in multiple comparisons. Categorical variables were tested using the chi-square test. The Kaplan-Meier and Cox proportional hazards regression analyses were performed to evaluate patient survival. In Kaplan-Meier analysis, RIC was dichotomized using the median value of all patients in the cohort. For Cox proportional hazards regression, all other relevant covariates, including isocitrate dehydrogenase 1 (IDH-1) mutation status, *O*-6-methylguanine-DNA methyltransferase (MGMT) promoter methylation status, sex, age, EOR, and CE volume, were considered. Patients who were alive at the last known follow-up were censored. The hypothesis of no effect was rejected at a 2-sided level of 0.05.

Results

Patients

A total of 136 patients were recruited. After surgery, 21 patients were excluded due to a nonglioblastoma pathology diagnosis. Due to their postoperative performance status, 84 (73.0%) of 115 patients received concurrent temozolomide chemoradiotherapy followed by adjuvant temozolomide (Stupp protocol). Other patients received short-course radiotherapy (17.4%, 20/115) or best supportive care (9.6%, 11/115). We only included the 84 patients who received the Stupp protocol for final analysis. Survival data were available for 80 (95.2%) of 84 patients and

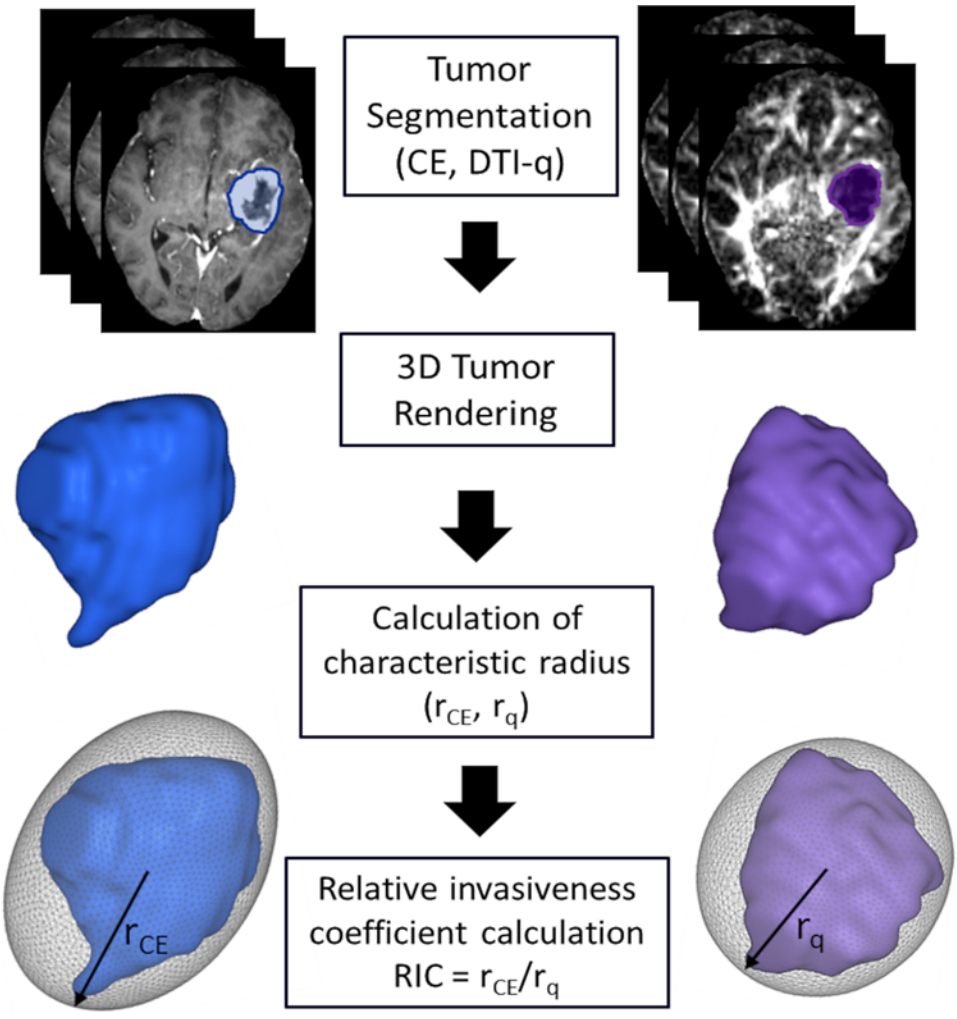

FIG. 2. A demonstration of calculation of the RIC. Tumor regions are segmented from postcontrast T1 (*left*) and DTI-q images (*right*), respectively. The smallest ellipsoids are fitted to the tumor volume. The characteristic radii of ROIs (r_{CE}, r_q) are calculated as the semimajor axis of ellipsoids. An RIC is calculated as the ratio of r_{CE}/r_q. Figure is available in color online only.

TABLE 1. Patient characteristics

Characteristic	Value
Total no. of patients	84
Males, n	62
Females, n	22
Mean age ± SD, yrs	57.3 ± 10.7
Complete resection, n	60
Partial resection, n	22
Biopsy, n	2
MGMT methylation positive, n (%)*	37 (45.1)
IDH-1 mutation positive, n (%)	7 (8.3)
Mean CE vol ± SD, cm^3	44.2 ± 27.2
Mean DTI-q abnormality vol ± SD, cm^3	43.8 ± 27.1
PFS (range), days	264 (25–1130)
OS (range), days	461 (52–1376)

* MGMT methylation status unavailable for 2 patients.

4 patients (4.8%) were lost to follow-up. Patient clinical characteristics are summarized in Table 1.

Tumor Volume and Characteristic Radius

The volumes of T1-weighted contrast-enhancement and DTI-q abnormalities are listed in Table 1. The mean (± SD) characteristic radii of the CE tumor region and DTI-q abnormalities were 3.6 ± 0.8 cm and 3.2 ± 0.8 cm, respectively.

Imaging Characteristics of Tumor Regions

In the comparison of rCBV, CE-ROI (2.52 ± 1.18, 95% confidence interval [CI] 2.25–2.80) had significantly higher rCBV values than q-ROI (2.08 ± 1.23, 95% CI 1.85–2.30, $p < 0.001$). For MRS comparisons, both tumor ROIs displayed abnormal metabolic signatures compared to the NAWM (all $p < 0.001$; Fig. 3). A full comparison is demonstrated in Supplementary Table 1.

Specifically, the choline/creatine (Cho/Cr) in q-ROI (0.66, 95% CI 0.63–0.70) was significantly higher than in

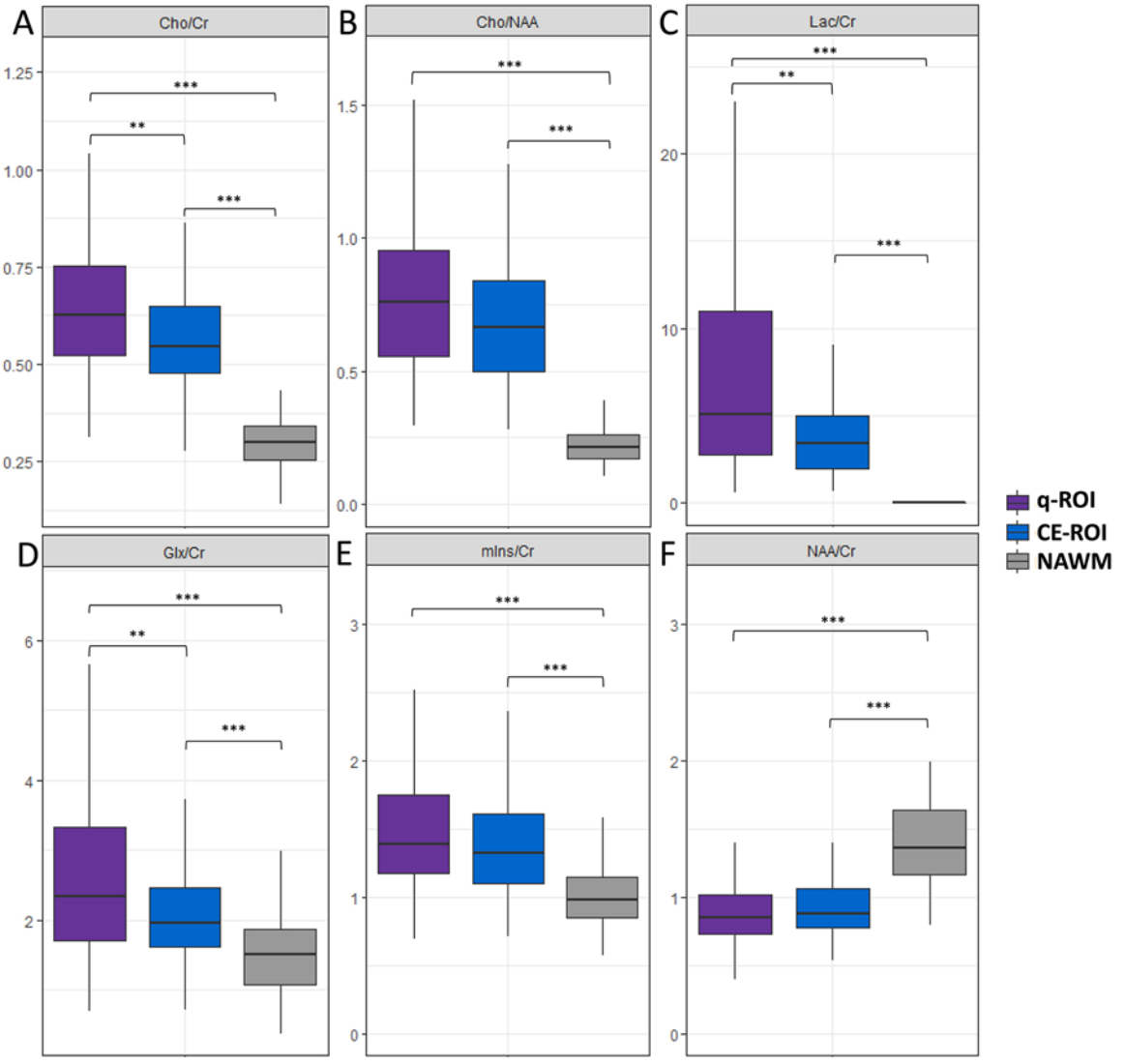

FIG. 3. Bar graphs of the metabolic signatures of ROIs. Both tumor ROIs display abnormal metabolic signatures. The q-ROI shows significantly higher levels of Cho/Cr, Lac/Cr, and Glx/Cr than CE-ROI. **p < 0.01, ***p < 0.001. Figure is available in color online only.

CE-ROI (0.56, 95% CI 0.54–0.59, p = 0.004). The lactate/creatine (Lac/Cr) in q-ROI (7.79, 95% CI 6.34–9.24) was significantly higher than in CE-ROI (4.17, 95% CI 3.49–4.85, p = 0.005). The glutamate + glutamine/creatine (Glx/Cr) in q-ROI (2.60, 95% CI 2.373–2.83) was significantly higher than in CE-ROI (2.08, 95% CI 1.94–2.22, p = 0.007).

Although not significant, the choline/*N*-acetylaspartate (Cho/NAA) ratio of q-ROI (0.84, 95% CI 0.75–0.92) was higher than in CE-ROI (0.75, 95% CI 0.63–0.87, p = 0.055). The myoinositol/creatine (mIns/Cr) ratio of q-ROI (1.59, 95% CI 1.44–1.73) was higher than in CE-ROI (1.45, 95% CI 1.33–1.56, p = 0.085). There was no significant difference between the NAA/Cr ratios of q-ROI (0.88, 95% CI 0.83–0.93) and CE-ROI (0.91, 95% CI 0.86–0.95, p = 0.171).

Patient Outcomes

The prognostic value of RIC was tested in multivariate survival models. The model of OS showed EOR (hazard ratio [HR] 2.32, 95% CI 1.20–4.44, p = 0.012), the volume of CE (HR 1.59, 95% CI 1.20–2.29, p = 0.007), and RIC (HR 1.40, 95% CI 1.06–1.85, p = 0.016) significantly affected OS. In multivariate modeling of progression-free survival (PFS), EOR (HR 3.27, 95% CI 1.67–6.38, p < 0.001) and RIC (HR 1.55, 95% CI 1.16–2.07, p = 0.003) significantly affected PFS.

We then dichotomized patients into 2 subgroups using the median value of RIC (0.89), with 42 patients in each group. The subgroup with an RIC > 0.89 had a significantly shorter survival than those with an RIC ≤ 0.89 (p = 0.001 for PFS, p = 0.002 for OS; Table 2, Fig. 4). No statistical difference was found between these 2 patient subgroups regarding age, sex, EOR, preoperative tumor volumes, or MGMT promoter methylation and IDH-1 mutation status (Table 2). Two case examples with an RIC ≤ 0.89 and an RIC > 0.89 are provided in Fig. 5.

TABLE 2. Clinical characteristics of the patient subgroups

Characteristic	RIC > 0.89	RIC ≤ 0.89	p Value
Mean age ± SD, yrs	58.1 ± 10.3	56.4 ± 11.1	0.661
Sex, n			0.457
Males	33	29	
Females	9	13	
EOR (of enhancing tumor)			0.883
Complete	29	30	
Partial	12	10	
Biopsy	1	1	
MGMT promoter methylation status*			0.183
Methylated	15	22	
Unmethylated	26	19	
IDH-1 mutation status			0.430
Mutant	2	5	
Wild-type	40	37	
Mean preop tumor vol ± SD, cm^3			
CE	48.3 ± 28.0	40.0 ± 14.7	0.291
DTI-q	41.5 ± 27.4	46.1 ± 26.7	0.263
Median survival (range), days			
OS	384 (52–839)	605 (25–1130)	**0.002†**
PFS	244 (37–550)	406 (135–1259)	**0.001†**

Boldface type indicates statistical significance.
* MGMT promoter methylation status unavailable for 2 patients.
† Log-rank test.

Discussion

In this study, we characterized CE and DTI-q abnormalities using multiparametric MRI and evaluated a proposed coefficient in assessing tumor invasiveness, which was calculated from the characteristic radii of CE and DTI-q abnormalities. The results showed that DTI-q abnormalities may represent a hypoxic tumor region. Integrating this coefficient into the survival model was useful in estimating tumor aggressiveness and predicting patient survival.

DTI-q and Tumor Regions With Abnormal Metabolic Signatures

Although providing useful structural information, conventional imaging is insufficient in reflecting tumor physiology.[19] The integration of advanced MRI techniques into clinical practice has been recommended for improving tumor volume targeting. Various findings support that DTI is useful in revealing tumor invasion and predicting patient survival.[9,18] In accordance with these studies, our current MRS results indicated that the q-ROI displayed abnormal metabolic signatures.

DTI-q and CE Represent Different Tumor Properties

In our results, the DTI-q abnormality showed a higher Cho/Cr ratio than the CE region, which implies that the DTI-q abnormality regions may have higher cellularity than CE regions, as Cho is regarded as a marker of cell membrane turnover.[12] The intensive tumor load in DTI-q abnormality may lead to hypoxia, which is supported by the significantly higher Lac/Cr level in DTI-q abnormality, compared to the CE region and normal control. The significantly elevated level of Glx, compared to the CE re-

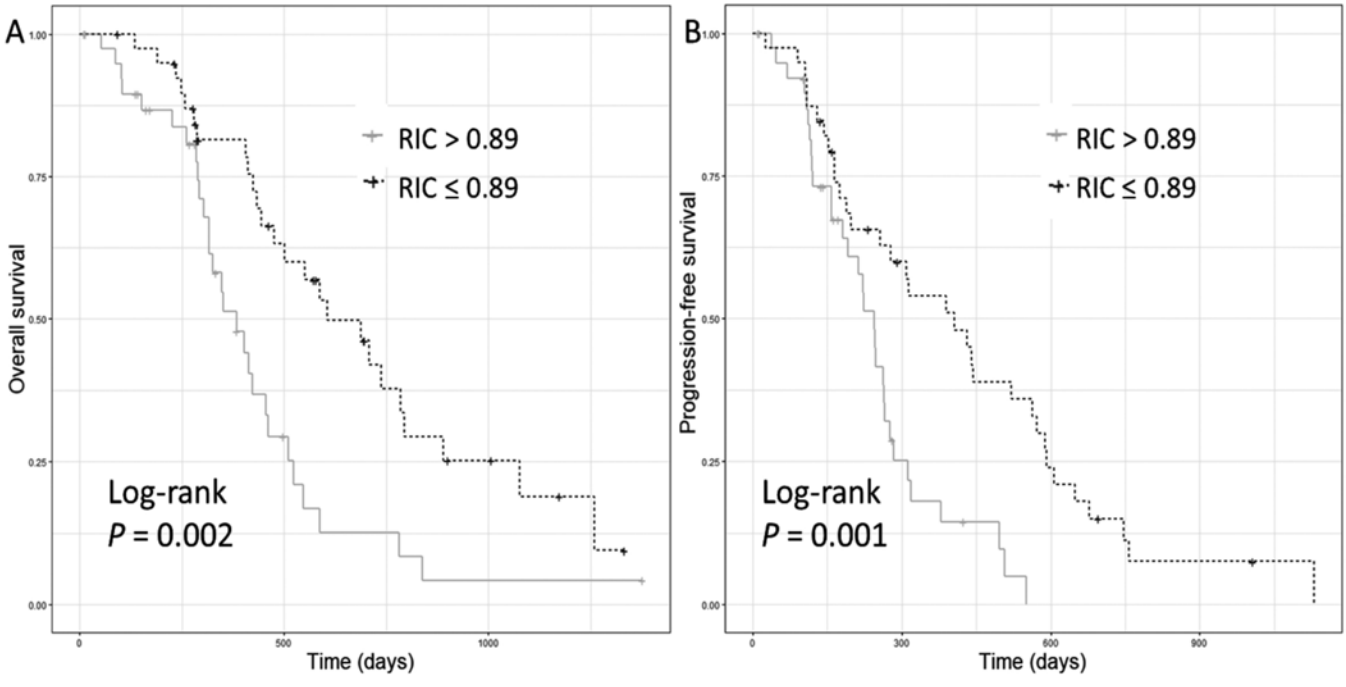

FIG. 4. Kaplan-Meier survival plots of patient clusters. The log-rank test showed patients with an RIC > 0.89 displayed worse OS (**A**, p = 0.002) and PFS (**B**, p = 0.001).

gion, also suggested the neuronal destruction and hypoxic microenvironment in the DTI-q abnormality region.[11,13] Compared to DTI-q abnormality, CE regions displayed a significantly elevated rCBV, which had a positive correlation with the MIB-1 index in a previous biopsy study.[17] This suggests that the CE tumor may indicate a proliferative front of the tumor.

RIC Combines DTI-q and CE Volumes

It is well known that hypoxia may be a driving force of tumor invasion and proliferation.[2] We hypothesized that the ratio of CE radius to DTI-q radius could indicate the tendency of tumor proliferation driven by hypoxia, which may potentially quantify tumor invasiveness. We tested this coefficient in the survival model and found clinical relevance with patient outcomes. Specifically, higher RIC may indicate a more aggressive tumor phenotype, in which the leading edge of proliferation runs further beyond the hypoxic core. It was previously reported that combining T1- and T2-weighted images is useful in quantifying tumor invasiveness.[26] Here we proposed our approach by integrating physiological imaging with structural imaging, which might potentially provide a more physiologically relevant measure.

Clinical Implications and Limitations

Our study may have neurosurgical implications. An extended EOR can significantly improve OS of the newly diagnosed glioblastoma.[21] The survival benefit from maximal safe resection is associated with not only extensive cytoreduction,[25] but also improvement of the efficacy of a temozolomide regimen.[24] Multiparametric MRI can facilitate the characterization of the multifaceted tumor properties. Our findings showed that DTI-q is an invasive region and that integrating CE and DTI-q volume may have prognostic value. Although the average volumes of CE and DTI-q abnormalities are similar, their locations and morphology can be different. In particular, for patients who have a greater extent of DTI-q abnormality than CE abnormality, a combination of both tumor areas into image-guided navigation may potentially bring benefits for maximal safe resection in surgical planning.

Our study had limitations. First, the resolution of CSI was lower than anatomical imaging and ^{1}H MRS voxels were larger than anatomical and physiological voxels. And second, our previous results have validated the imaging markers using histological assessment and longitudinal observations; further biological studies may be needed for future clinical application.

Conclusions

The imaging characteristics of DTI-q abnormality suggest that it is a hypoxic region with a high tumor burden. Integrating the extent of DTI-q and CE regions into clinical practice may bring benefits for patient care.

Acknowledgments

The research was supported by the National Institute for Health Research (NIHR) Brain Injury MedTech Co-operative based at Cambridge University Hospitals NHS Foundation Trust and University of Cambridge. The views expressed are those of the authors and not necessarily those of the NHS, the NIHR, or the Department of Health and Social Care (S.J.P., project reference NIHR/CS/009/011). In addition, this work was supported by a CRUK core grant (no. C14303/A17197 and A19274, F.M. laboratory); Cambridge Trust and China Scholarship Council (C.L. and S.W.); the Chang Gung Medical Foundation and Chang Gung Memorial Hospital, Keelung, Taiwan (J.L.Y.); CRUK & EPSRC Cancer Imaging Centre in Cambridge and Manchester (F.M. and T.T., grant no. C197/A16465); the NIHR Cambridge Biomedical Research Centre (T.M. and S.J.P.); and the Commonwealth Scholarship Commission and Cambridge Commonwealth Trust (N.R.B.).

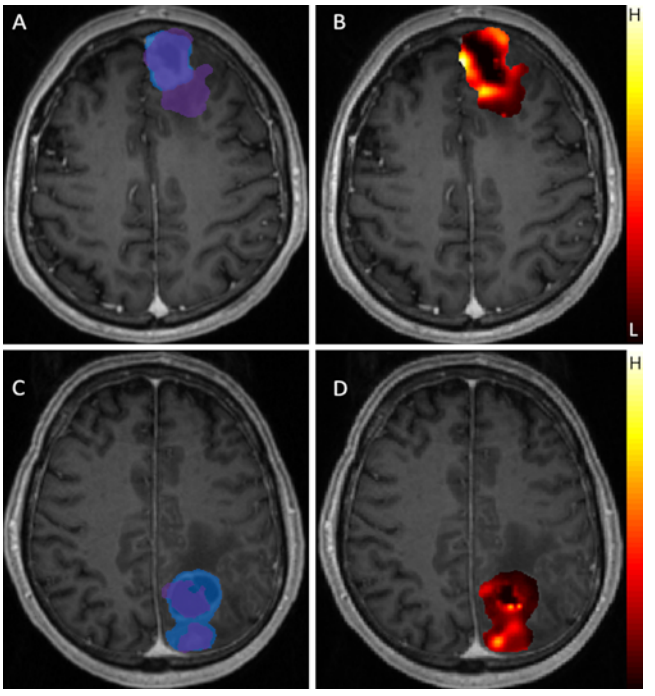

FIG. 5. Two case examples of tumor invasiveness revealed by CE tumor regions and DTI-q abnormalities. **A and B:** Case 1 is a 64-year-old man, with a CE tumor of 62.6 cm^3 and RIC of 0.81. **C and D:** Case 2 is a 69-year-old man, with a CE tumor of 31.2 cm^3 and RIC of 1.31. A and C indicate the CE-ROI (*blue*) and q-ROI (*purple*) in each case. B and D indicate the rCBV maps on a voxel-wise basis across the CE-ROI and q-ROI. Both patients received tumor resection with the guidance of neuronavigation and 5-ALA fluorescence for maximal resection. Complete resection was achieved in both patients according to the 72-hour postoperative MR images. Pathological assessment confirmed both were MGMT promoter unmethylated and IDH-1 wild-type glioblastomas. Both patients received concomitant and adjuvant temozolomide chemoradiotherapy following the Stupp protocol. The PFS and OS of case 1 were 563 and 697 days, respectively. The PFS and OS of case 2 were 159 and 317 days, respectively. Figure is available in color online only.

References

1. Behrens TE, Woolrich MW, Jenkinson M, Johansen-Berg H, Nunes RG, Clare S, et al: Characterization and propagation of uncertainty in diffusion-weighted MR imaging. **Magn Reson Med 50:**1077–1088, 2003
2. Colwell N, Larion M, Giles AJ, Seldomridge AN, Sizdahkhani S, Gilbert MR, et al: Hypoxia in the glioblastoma microenvironment: shaping the phenotype of cancer stem-like cells. **Neuro Oncol 19:**887–896, 2017
3. Hegi ME, Diserens AC, Gorlia T, Hamou MF, de Tribolet N,

Weller M, et al: MGMT gene silencing and benefit from temozolomide in glioblastoma. **N Engl J Med 352:**997–1003, 2005
4. Kaur B, Khwaja FW, Severson EA, Matheny SL, Brat DJ, Van Meir EG: Hypoxia and the hypoxia-inducible-factor pathway in glioma growth and angiogenesis. **Neuro Oncol 7:**134–153, 2005
5. Kreis R: Issues of spectral quality in clinical ^{1}H-magnetic resonance spectroscopy and a gallery of artifacts. **NMR Biomed 17:**361–381, 2004
6. Li C, Wang S, Yan JL, Piper RJ, Liu H, Torheim T, et al: Intratumoral heterogeneity of glioblastoma infiltration revealed by joint histogram analysis of diffusion tensor imaging. **Neurosurgery** [epub ahead of print], 2018
7. Li C, Yan JL, Torheim T, McLean MA, Boonzaier NR, Huang Y, et al: Low perfusion compartments in glioblastoma quantified by advanced magnetic resonance imaging: correlation with patient survival. **bioRxiv** [epub ahead of print], 2017
8. Li YM, Suki D, Hess K, Sawaya R: The influence of maximum safe resection of glioblastoma on survival in 1229 patients: can we do better than gross-total resection? **J Neurosurg 124:**977–988, 2016
9. Mohsen LA, Shi V, Jena R, Gillard JH, Price SJ: Diffusion tensor invasive phenotypes can predict progression-free survival in glioblastomas. **Br J Neurosurg 27:**436–441, 2013
10. Moshtagh N: **Minimum Volume Enclosing Ellipsoid.** (https://pdfs.semanticscholar.org/21c3/072e516c93b28ccd06f5b994998abc517a7f.pdf) [Accessed February 25, 2019]
11. Noch E, Khalili K: Molecular mechanisms of necrosis in glioblastoma: the role of glutamate excitotoxicity. **Cancer Biol Ther 8:**1791–1797, 2009
12. Padhani AR, Miles KA: Multiparametric imaging of tumor response to therapy. **Radiology 256:**348–364, 2010
13. Pardon MC, Yanez Lopez M, Yuchun D, Marjańska M, Prior M, Brignell C, et al: Magnetic resonance spectroscopy discriminates the response to microglial stimulation of wild type and Alzheimer's disease models. **Sci Rep 6:**19880, 2016
14. Peña A, Green HAL, Carpenter TA, Price SJ, Pickard JD, Gillard JH: Enhanced visualization and quantification of magnetic resonance diffusion tensor imaging using the p:q tensor decomposition. **Br J Radiol 79:**101–109, 2006
15. Potgieser ARE, Wagemakers M, van Hulzen ALJ, de Jong BM, Hoving EW, Groen RJM: The role of diffusion tensor imaging in brain tumor surgery: a review of the literature. **Clin Neurol Neurosurg 124:**51–58, 2014
16. Price SJ, Gillard JH: Imaging biomarkers of brain tumour margin and tumour invasion. **Br J Radiol 84:**S159–S167, 2011
17. Price SJ, Green HAL, Dean AF, Joseph J, Hutchinson PJ, Gillard JH: Correlation of MR relative cerebral blood volume measurements with cellular density and proliferation in high-grade gliomas: an image-guided biopsy study. **AJNR Am J Neuroradiol 32:**501–506, 2011
18. Price SJ, Jena R, Burnet NG, Carpenter TA, Pickard JD, Gillard JH: Predicting patterns of glioma recurrence using diffusion tensor imaging. **Eur Radiol 17:**1675–1684, 2007
19. Price SJ, Jena R, Burnet NG, Hutchinson PJ, Dean AF, Peña A, et al: Improved delineation of glioma margins and regions of infiltration with the use of diffusion tensor imaging: an image-guided biopsy study. **AJNR Am J Neuroradiol 27:**1969–1974, 2006
20. Price SJ, Young AMH, Scotton WJ, Ching J, Mohsen LA, Boonzaier NR, et al: Multimodal MRI can identify perfusion and metabolic changes in the invasive margin of glioblastomas. **J Magn Reson Imaging 43:**487–494, 2016
21. Sanai N, Polley MY, McDermott MW, Parsa AT, Berger MS: An extent of resection threshold for newly diagnosed glioblastomas. **J Neurosurg 115:**3–8, 2011
22. Smith SM, Jenkinson M, Woolrich MW, Beckmann CF, Behrens TEJ, Johansen-Berg H, et al: Advances in functional and structural MR image analysis and implementation as FSL. **Neuroimage 23 (Suppl 1):**S208–S219, 2004
23. Sternberg EJ, Lipton ML, Burns J: Utility of diffusion tensor imaging in evaluation of the peritumoral region in patients with primary and metastatic brain tumors. **AJNR Am J Neuroradiol 35:**439–444, 2014
24. Stummer W, Meinel T, Ewelt C, Martus P, Jakobs O, Felsberg J, et al: Prospective cohort study of radiotherapy with concomitant and adjuvant temozolomide chemotherapy for glioblastoma patients with no or minimal residual enhancing tumor load after surgery. **J Neurooncol 108:**89–97, 2012
25. Stummer W, Pichlmeier U, Meinel T, Wiestler OD, Zanella F, Reulen HJ: Fluorescence-guided surgery with 5-aminolevulinic acid for resection of malignant glioma: a randomised controlled multicentre phase III trial. **Lancet Oncol 7:**392–401, 2006
26. Swanson KR, Rostomily RC, Alvord EC Jr: A mathematical modelling tool for predicting survival of individual patients following resection of glioblastoma: a proof of principle. **Br J Cancer 98:**113–119, 2008
27. Vogelbaum MA, Jost S, Aghi MK, Heimberger AB, Sampson JH, Wen PY, et al: Application of novel response/progression measures for surgically delivered therapies for gliomas: Response Assessment in Neuro-Oncology (RANO) Working Group. **Neurosurgery 70:**234–244, 2012
28. Wen PY, Macdonald DR, Reardon DA, Cloughesy TF, Sorensen AG, Galanis E, et al: Updated response assessment criteria for high-grade gliomas: response assessment in neuro-oncology working group. **J Clin Oncol 28:**1963–1972, 2010
29. Yan JL, van der Hoorn A, Larkin TJ, Boonzaier NR, Matys T, Price SJ: Extent of resection of peritumoral diffusion tensor imaging-detected abnormality as a predictor of survival in adult glioblastoma patients. **J Neurosurg 126:**234–241, 2017

Disclosures

The authors report no conflict of interest concerning the materials or methods used in this study or the findings specified in this paper.

Author Contributions

Conception and design: Li, Yan, Markowetz. Acquisition of data: Li, Yan, Boonzaier, Matys, Price. Analysis and interpretation of data: Li, Wang, Yan, Boonzaier. Drafting the article: Li, Yan, Sinha. Critically revising the article: Li, Wang, Boonzaier, Torheim, Sinha, Matys, Price. Reviewed submitted version of manuscript: Li, Wang, Boonzaier, Torheim, Sinha, Matys, Price. Approved the final version of the manuscript on behalf of all authors: Li. Statistical analysis: Li, Wang, Yan, Boonzaier, Torheim, Markowetz. Administrative/technical/material support: Li, Torheim, Markowetz. Study supervision: Markowetz, Price.

Online-Only Content

Supplemental material is available with the online version of the article.

Supplementary Table 1. https://thejns.org/doi/suppl/10.3171/2019.2.JNS182620.

Correspondence

Chao Li: University of Cambridge, United Kingdom. cl109@outlook.com.